

Water Cherenkov Detectors for High-Energy Gamma-Ray Astronomy

Celine Beier

12.04.2023

Contents

1	Introduction	2
2	The Milagro Experiment	6
3	The HAWC Experiment	14
4	The LHAASO Experiment	21
5	The SWGO Experiment	24
6	Conclusion	25
7	Bibliography	26

1 Introduction

High-Energy Gamma-Ray Astronomy

High-energy gamma-ray astronomy is the study of photons from astrophysical sources with energies above 100MeV . Their production can be divided in leptonic and hadronic processes. Leptonic processes include the emission of photons in synchrotron and bremsstrahlungs radiation or the inverse Compton effect, where a photon's energy is increased by scattering with a high-energy lepton. Hadronic gamma-ray production involves the nuclear interaction of high-energy protons and nuclei with interstellar medium in which neutral hadrons like π^0 mesons are produced. These mesons then decay into high-energy gamma-rays. [1]

High-energy gamma-rays are messengers from the astrophysical sources in which they are produced and their study allows for the investigation of these objects. Within our galaxy, sources of gamma-rays are pulsars, pulsar wind nebulae, supernova remnants and the galactic center, while outside of our galaxy there are starburst galaxies, active galactic nuclei and gamma-ray bursts. [1]

Gamma-rays can be created from cosmic rays, for example through the production of synchrotron radiation in magnetic fields. Accordingly, they are linked to the study of cosmic rays, their origins and mechanisms for particle acceleration and particle transport in the universe. Cosmic rays are charged particles, like protons, electrons, positrons or heavy ions, with energies from 10^9eV to 10^{20}eV , which are produced in galactic and extra-galactic astrophysical sources. Since they consist out of charged particles, they are deflected by magnetic fields and so the reconstruction of the source from cosmic rays reaching earth is almost impossible. However, gamma-rays produced from cosmic rays will arrive at earth straight from the source and therefore are useful tools in investigating comic rays. [1, 2]

Studying high-energy gamma-rays can also be a mean to probe physics beyond the Standard Model: For example, some dark matter models describe dark matter as massive, weakly interacting particles which are their own anti-particles. When they annihilate in dark matter dense regions of the universe, they could produce high-energy photons. Other dark matter models include high-energy gamma-rays as decay products of dark matter particles. [1]

Similarly, new phenomena in fundamental physics that affect the creation and propagation of photons can be probed with high-energy gamma-rays. For example, some theories of quantum gravitation include a violation of Lorentz invariance which would affect photon propagation and observations of gamma-rays have placed constraints on those theories. [1]

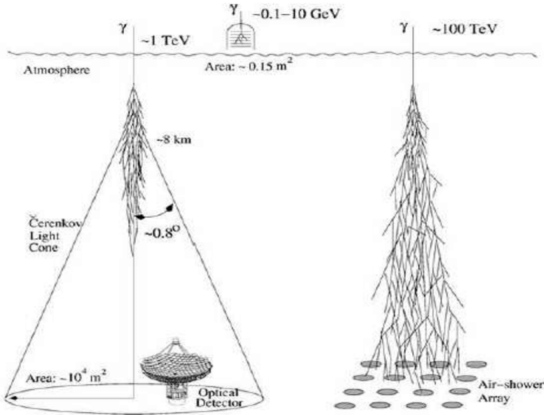


Figure 1: Schematic view of different high-energy gamma-ray detection methods including satellite detectors, EAS arrays and Atmospheric Cherenkov telescopes with the respective energy limits. From [2]

Detectors for High-Energy Gamma-Rays

High-energy gamma-ray astronomy faces several experimental challenges: Gamma-rays arriving at earth have a large energy range from MeV upwards which needs to be covered by detectors. Their flux is very small, about $2 \cdot 10^{-11} photons/(cm^2 s)$ for a point source like the Crab Nebula, and decreases according to a power law with increasing energy:

$$\frac{dN}{dE} \propto E^{-\gamma}$$

with $\gamma \sim 2 - 3$. The background from cosmic rays is about 10^3 to 10^4 times larger and additionally, earth's atmosphere is opaque to gamma-rays, so at ground-level, gamma-rays cannot be directly detected. [2]

Different methods for high-energy gamma-ray astronomy are illustrated in figure 1. The only option for direct detection of gamma-rays is through detectors on satellites. These rely on the conversion of the gamma-ray photons into electron-positron pairs (at high energies other energy loss processes like the photoelectric effect and Compton scattering are insignificant) which are then tracked to allow for the reconstruction of the primary particle direction. An absorption calorimeter is used to measure and reconstruct the primary particle energy. Examples of satellite detector experiments include COS-B, EGRET and the Fermi Gamma-Ray Space Telescope. Satellite detectors might be the most direct detection technique for gamma rays, but are very limited in their volume and mass. Accordingly, they have a small collection area which sets a maximum energy limit of about $10GeV$ above which no statistically significant detections can be made. [2, 3]

When gamma-rays hit earth's atmosphere electromagnetic showers are induced: The

photon interacts with particles in the atmosphere and creates an electron-positron pair, which will emit bremsstrahlung. These two processes, electron-positron creation and the emission of bremsstrahlungs photons, continue creating a particle cascade until the electron energy falls below the critical energy at which point the remaining energy is dissipated through ionization. The secondary particles in this extensive air shower (EAS) can be probed by ground-based detectors. [2]

EAS arrays detect secondary shower particles with scintillation detectors. They are composed of small individual plastic scintillation counters with an area of about $1m^2$ each which are arranged in an arrays covering between $40,000m^2$ and $230,000m^2$. The active detection area is often less than 1% of the total array area and only a small amount of particles in an air shower are usually detected. This leads to a high energy threshold of about $100TeV$. EAS arrays have a large field-of-view of about $2sr$ and can operate in every weather which gives them a high duty factor close to 100%. Examples of former EAS array experiments are CYGNUS and CASA, while Tibet-AS γ and ARGO, which uses resistive plate chambers instead of plastic scintillators, are still running. [4]

Besides EAS arrays the secondary particles in an air shower can be probed by measuring the Cherenkov light they emit. A particle moving in a medium produces Cherenkov light if its velocity exceeds the speed of light in the medium

$$v > \frac{c}{n}$$

where n is the refractive index of the medium. The passing particle will polarize atoms in the medium and in the de-excitation process electromagnetic radiation will be emitted. This Cherenkov light is emitted at an angle θ with [2]

$$\cos(\theta) = \frac{c}{nv}$$

Atmospheric Cherenkov telescopes (ACT) detect the Cherenkov radiation secondary EAS particles produce in the atmosphere. They usually consist of a parabolic or spherical mirror with a diameter of around $10m$ that focuses the incoming photons onto a tightly packed array of photomultiplier tubes (PMT). Several of these telescopes are clustered in an array with a respective distance of about $100m$ which allows for a large detection area of 10^5m^2 . ATCs have a relatively low energy-threshold of about $100GeV$ and can cover an energy range up to about $50TeV$. They usually have very effective background rejection of hadronic showers induced by cosmic rays relying on the different shapes of Cherenkov light and good angular ($\approx 0.1^\circ$) and energy ($\approx 15\%$) resolution. Disadvantages include that ATCs usually

operate at a small field of view and can therefore only observe one gamma-ray source at a time. Since they are optical detectors they can only operate in good weather (dark, clear nights) and so they have a small duty factor of about 10%. Examples of ongoing ACT experiments include the HESS Observatory in Namibia, the VERITAS experiment in Arizona, which was preceeded by Whipple, and the MAGIC experiment (preceeded by HEGRA) on the Canary Islands. [2, 3]

Water Cherenkov detectors (WCD) were developed in the late 1990s with the intention of combining the advantages of the two previously existing detection techniques: Water Cherenkov detectors can have a relatively low energy threshold like ACTs while simultaneously maintaining a very high duty factor close to 100% and large field of view like EAS arrays. They consist of a large volume of water in which secondary particles from an EAS produce Cherenkov light which PMTs will detect. From the characteristics of the Cherenkov light the energy and the direction of the primary particle can be reconstructed and the signal electromagnetic showers can be distinguished from background hadronic showers. The first water Cherenkov detector was the Milagro experiment, which was succeeded by HAWC, which is still collecting data for physics analysis. Currently, two more water Cherenkov detectors, LHHASO and SWGO, are being planned and built. [2, 3]

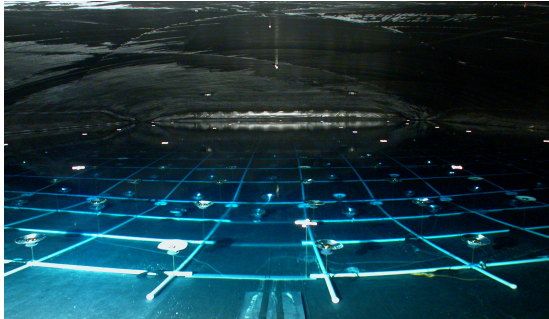


Figure 2: Photograph of the Milagro experiment. From [8]

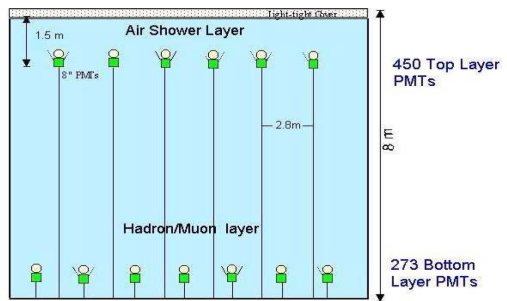


Figure 3: Schematic view of the Milagro experiment. From [3]

2 The Milagro Experiment

Milagro was the first water Cherenkov detector for EAS induced by high-energy gamma-rays. It was build in 1999 by a collaboration of US-American universities and research institutes and started taking data for physics analysis in 2000. The experiment underwent a major upgrade in 2004 when the outrigger array was installed to improve the angular and energy resolution. In 2008, Milagro was dismantled and its component were re-used for the next-generation water Cherenkov detector, HAWC. [5, 6, 7]

Detector Setup

The Milagro experiment (figure 2) is located in the Jemez Mountains in New Mexico at an altitude of 2650m. It was build into an existing frustum-shaped pond with a rectangular surface area of 60m x 80m and a height of 8m . The pond is covered with a light-tight barrier to eliminate background light and filled with 24 million liters of water in which two layers of upwards pointing photomultiplier tubes (PMT) are submerged (figure 3). Milagro uses 723 Hamamatsu R5912 10-stage PMTs with a diameter of 20cm which are anchored to the ground by strings and float in the water. [3]

The upper layer of 450 PMTs is located 1.5m under water which corresponds to about 4 radiation lengths. These PMTs, called the shower layer, are used for triggering the detector read-out and for measuring the arrival time and density of the shower front. The bottom area of the pond is smaller than the top and accordingly only covered by 273 PMTs. This second PMT layer is 6m (16 radiations lengths) below the surface and is called the hadron/muon layer as it is used to differentiate gamma-ray-induced EAS from background hadron-induced showers. It also provides additional measurements for the shower's energy. [3, 6, 9]

The PMTs in Milagro are about $3m$ apart from each other. Cherenkov light in water propagates in a cone with a large opening angle of about 42° and therefore this array of PMTs is enough to provide complete coverage of the pond. [3]

Background Rejection

An experimental challenge for ground-based gamma-ray astronomy are showers induced by cosmic rays which can outnumber gamma-ray showers by a factor of 10^3 to 10^4 . The background rejection in Milagro relies on information from the hadron/muon layer. For an electromagnetic shower from a gamma-ray, these PMTs will be illuminated by uniform, low level of light as most shower particles are attenuated in the water above. In contrast, hadronic showers induced by cosmic rays typically contain particles that are able to deeply penetrate into the water, like muons or hadrons. They will produce Cherenkov light that the PMTs register as high-intensity, strongly localized light deposits. Typical hadron- and photon-induced events can be seen in figure 4. [6]

To quantify this shower behavior the compactness factor (C-value) is defined as the ratio of the number of PMTs in the bottom layer measuring at least 2 photoelectrons (PE) and the brightest PMT in the bottom layer measured in units of photoelectrons:

$$C = \frac{N_{PMT \geq 2PE}}{PE_{max}}$$

Gamma-ray-induced showers will have large C-values, while hadronic showers have small C-values, this is illustrated for simulated and measured events in figure 5. For data analysis, events with a C-value ≤ 2.5 are disregarded, which corresponds to a background rejection efficiency of 90% while 50% of gamma-ray induced events are retained. [6]

The original draft of the Milagro experiment featured 3 layers of PMTs (figure 6). While the shower layer was implemented as planned, the bottom PMT array was originally meant to be split into a hadron layer and a muon layer. The hadron layer would have had upwards pointing PMTs to detect deeply-penetrating particles in hadronic showers, but also catch the tails of electromagnetic showers for calorimetric measurements. About $1m$ above the pond bottom an opaque barrier would have shielded the third layer of PMTs, the muon layer, from all downward coming Cherenkov light. These PMTs were supposed to probe the presence of muons in a shower by observing Cherenkov light produced by them in a diffusing cell around each PMT. Since muons are unique to hadronic showers, the detection of a muon would have unambiguously identified a shower as hadronic and therefore this third

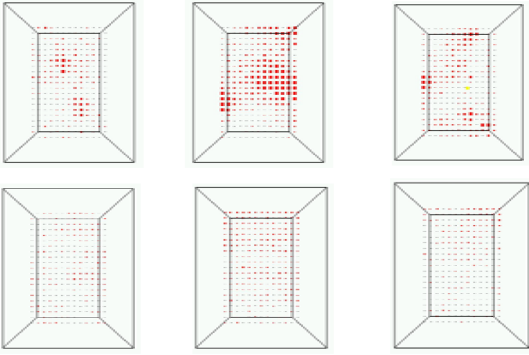


Figure 4: Typical hadronic (top row) and electromagnetic (bottom row) showers in the hadron/muon layer. The area of a square is proportional to the intensity measured by a PMT at that location. From [6]

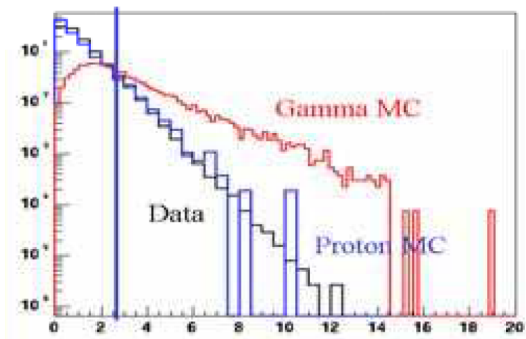


Figure 5: C-value distribution for data and simulated photon- and hadron-induced showers. The vertical blue line indicates the background cut of $C \leq 2.5$. From [6]

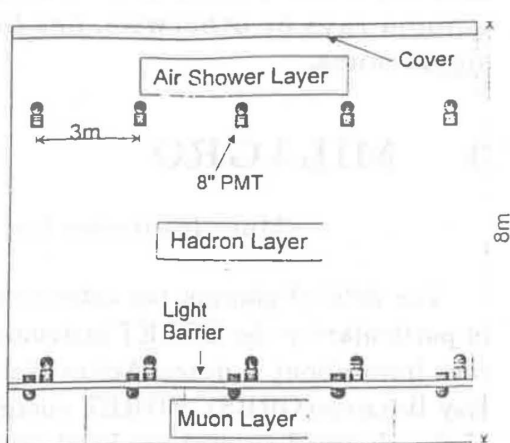
layer, which got never build for financial reasons, could have improved the background rejection capabilities. [5]

Data Processing

The data-acquisition system is triggered when 60 or more PMTs sense light within a coincidence window of 200ns . This corresponds to an event rate of 1700Hz . For each event, the arrival time and pulse intensity (number of photoelectrons) for each PMT is recorded. The raw data is reconstructed in real time and shower core position, shower direction, shower size and parameters used for photon-hadron separation are calculated; only events of interest are permanently saved. [3, 6]

When a high-energy gamma-ray or cosmic ray hits the atmosphere and creates a shower, the produced secondary particles will be highly relativistic and accordingly will be moving in approximately the same direction as the primary particle. The shower front of an EAS is therefore perpendicular to the direction of the primary particle. The relative arrival times of Cherenkov radiation at the PMTs can be used to create a recording of the shower front (figure 7) which is fit using a least-squares fit; early Milagro result use a simple plane while later data processing uses more complex shower-front models as the fit function. From the shower-front the primary particle direction can be reconstructed. [3]

The statistical uncertainty in the direction of the primary particle can be estimated by dividing the shower PMT array into two overlapping arrays of equal size. The difference between the independently reconstructed directions from the sub-arrays (figure 9) is twice as large as the angular resolution of the whole detector. However,



MILAGRO

Figure 6: Schematic view of an early draft of the Milagro experiment featuring three layers of PMTs. From [5]

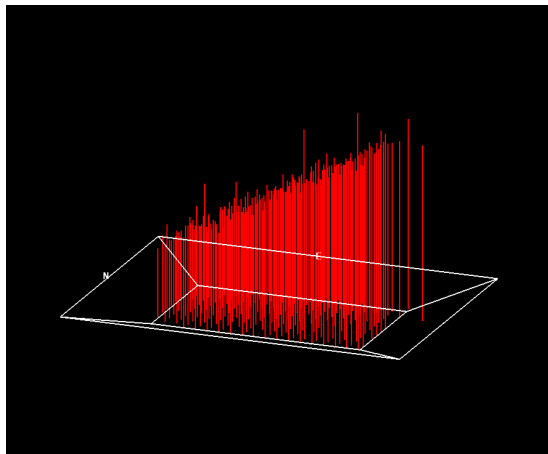


Figure 7: In this arrival time distribution the line height is proportional to the relative time Cherenkov light was detected at the respective PMT. Only the top layer PMT responses are shown. From [8]

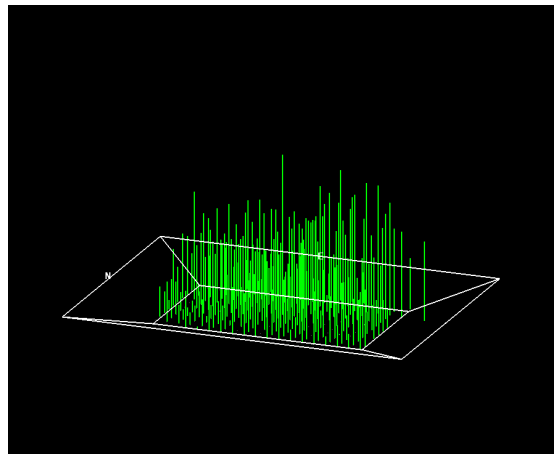


Figure 8: In this pulse intensity distribution the line height is proportional to the amount of light arriving at the PMTs. The event is the same as in figure 7. Only the top layer PMT responses are shown. From [8]

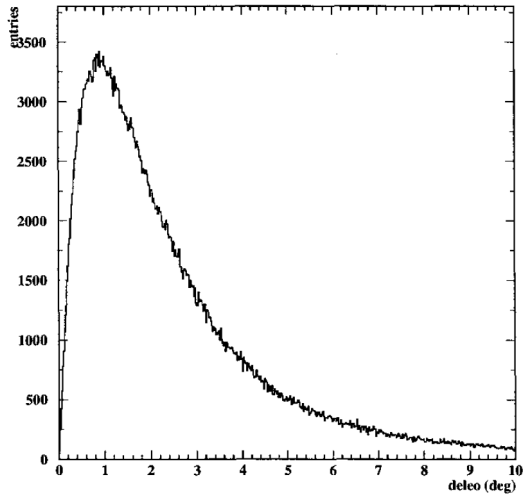


Figure 9: The angular resolution is estimated by dividing the shower array into two sub-arrays. Plotted is the angular difference between the two independent shower reconstructions. From [10]

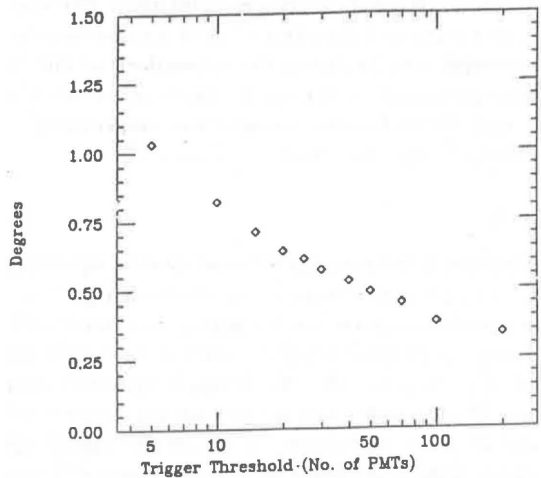


Figure 10: Angular resolution in dependence of the number of PMTs used in the fit. On average, the angular resolution is 0.75° . From [5]

the angular resolution also depends on the number of PMTs used to fit the shower front (figure 10). On average, Milagro's angular resolution is 0.75° . [9, 10]

The energy of the primary particle can be reconstructed from the intensity and distributions of the PMT signals in the two layers (figure 8) using a calibrated correlation of the primary particle energy with the C-value. Milagro is able to measure the energy deposited in its pond with a resolution of about 30%, however, fluctuations in the longitudinal shower development and uncertainties in the reconstruction algorithms result in a resolution of the primary particle energy that is much larger. The primary particle energy reconstruction heavily depends on the ability to precisely locate the shower core: With access to only the information from the PMTs in the pond, a low energy shower with a shower core close or in the pond will appear the same as a high-energy shower with a core far from the pond. To allow for a better determination of the shower core, Milagro was updated in 2004 with the outrigger array. [3, 6]

Outrigger array

Milagro's outrigger array consists of 175 individual water Cherenkov detectors covering a total area of $40,000m^2$ around the pond (figure 11). Each detector is made out of a $2000l$ water tank with an area of $4.6m^2$ and a height of $1m$ (figure 12). The inside is lined with a reflective plastic and a single PMT is placed centered on

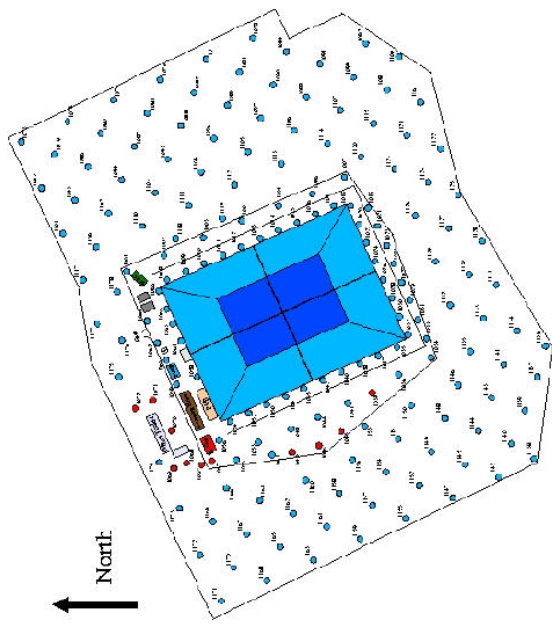


Figure 11: Locations of the 175 outrigger detectors in a $40,000m^2$ area around the Milagro pond. From [8]

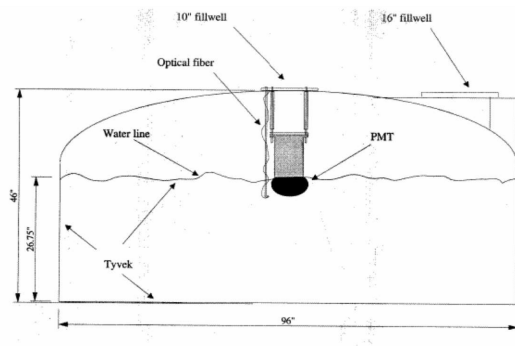


Figure 12: Cross-section of an outrigger detector consisting of a $2000l$ water tank and a single PMT. From [11]

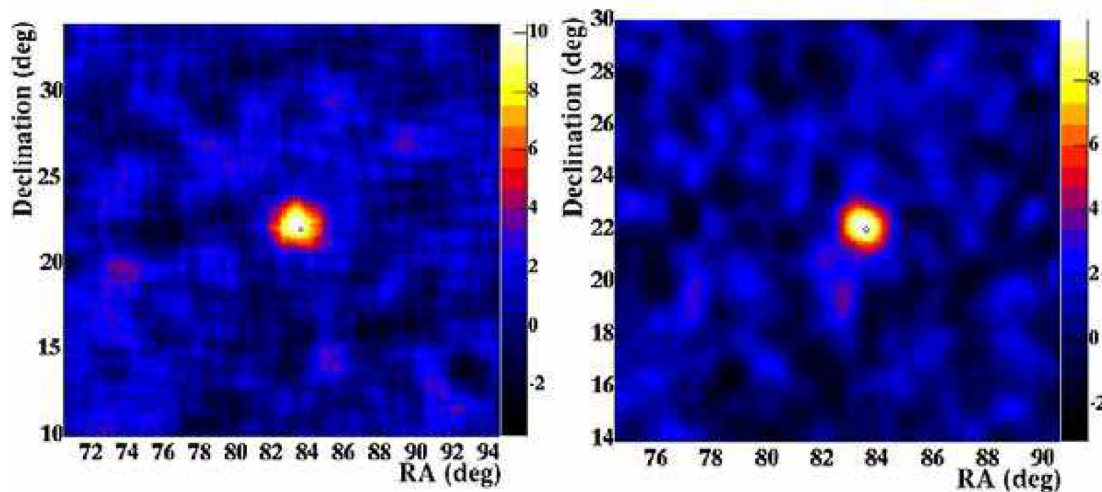


Figure 13: Signal from the Crab Nebula before (left) and after (right) the installation of the outrigger array which improves the angular resolution from an average of 0.75° to 0.4° . From [6]

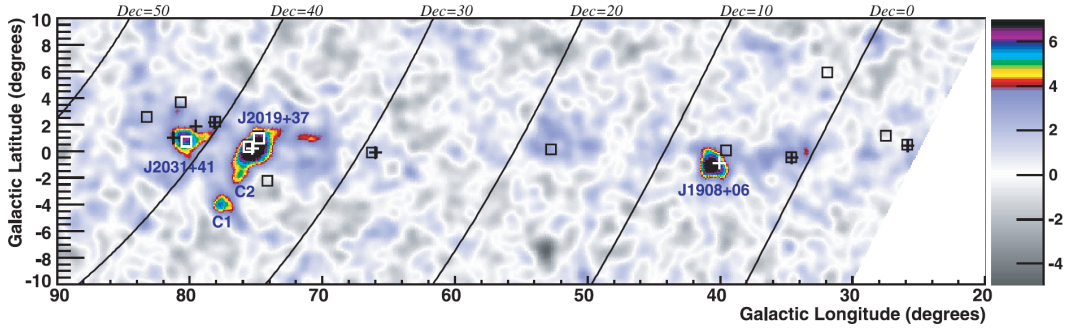


Figure 14: Map of the Galactic plane with the high-energy gamma-ray sources observed by Milagro. The color represents the significance in standard deviations and boxes indicate the locations of sources observed by EGRET. From [13]

top of the tank. The installation of the outrigger array increases Milagro's ability to locate shower cores and allows for the precise reconstruction of EAS with cores up to 100m away from the pond. The additional information improves the energy resolution and the average angular resolution from 0.75° to 0.4° (figure 13). [6]

Scientific Results

Milagro confirmed and improved observations from other high-energy gamma-ray experiments (figure 14). In particular, Milagro detected 14 of the 34 galactic TeV gamma-ray sources seen by the Fermi Gamma-Ray Space Telescope and was able to extend the observation far above the satellite's energy limit. It also discovered several new TeV gamma-ray sources and made the first observation of gamma-rays sources with a large angular extend (figure 15). [12, 13, 14]

Another significant result from Milagro was the observation of the galactic diffuse gamma-ray emission near $10TeV$ (figure 16). Comparing the measured results to models of gamma-ray production showed that in the TeV energy regime the diffuse gamma-ray emission is largely produced by leptonic processes, especially the inverse Compton effect where cosmic microwave background photons scatter off high-energetic electrons of about $100TeV$. This survey also revealed a so-far unexplained TeV gamma-ray excess in the Cygnus region. [15]

During its eight years of operation, Milagro collected a data set of more than 95 billion cosmic ray events, which was the largest such data set at the time. In its analysis, an unexpected anisotropy in the cosmic ray arrival directions was discovered (figure 17), which has yet to be explained. [16]

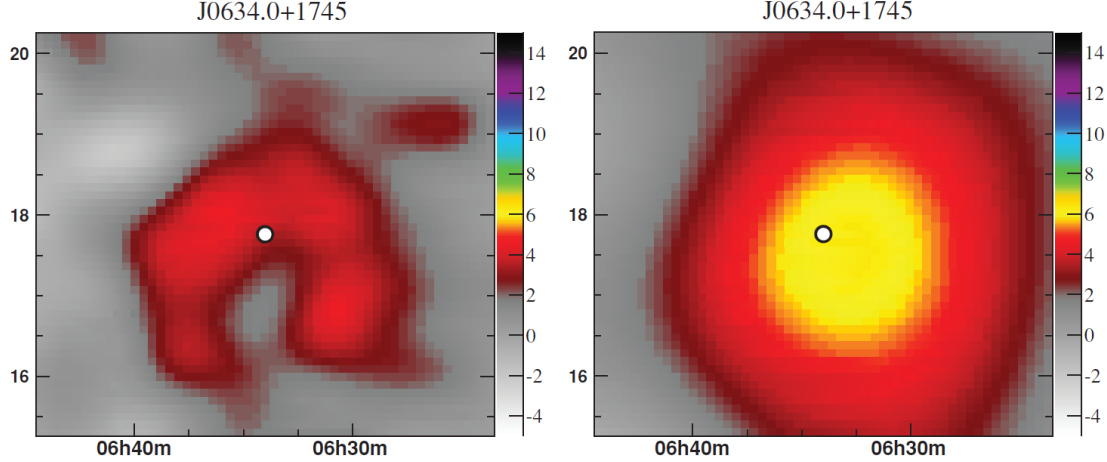


Figure 15: Milagro significance map around the high-energy gamma-ray source J0634.0+1745. The location of the sources as observed by the Fermi Gamma-Ray Space Telescope is identified by the white dot. On the left, the significance map is smoothed by a point-spread function, on the right additionally with a 1° Gaussian function. From [14]

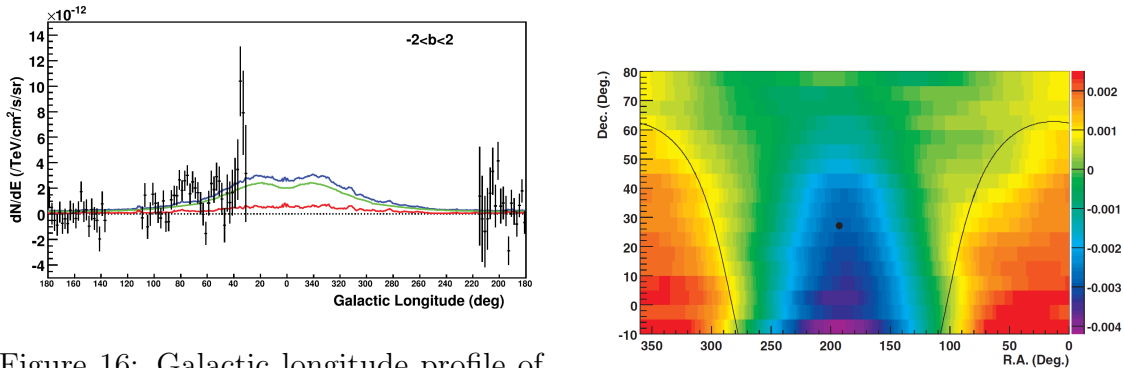


Figure 16: Galactic longitude profile of the diffuse gamma-ray emission around 10TeV in the galactic plane. The black data was measured by Milagro while the blue line represents the predicted flux according to the GALPROP model with hadronic (red) and leptonic (green) production processes. The excess around 40° is so far unexplained. From [15]

Figure 17: Cosmic ray anisotropy as observed by Milagro with the colors indicating the deviation from the expected isotropic distribution. The field shown corresponds to the viewfield of Milagro, not the full sky. From [16]

3 The HAWC Experiment

The **H**igh **A**ltitude **W**ater Cherenkov (HAWC) experiment was build in 2015 by a collaboration from US-American and Mexican universities. Data-taking with the detector started in 2016 and is still on-going. The experiment underwent a major upgrade in 2018 when the outrigger array was installed. [17, 18]

From Milagro to HAWC

The Milagro experiment was the first water Cherenkov detector and its design was largely influenced by the boundary conditions set by the pond that was build for a previous geothermal energy project which became the main detector. [3] Based on the success of Milagro, the HAWC experiment was meant to be the next-generation water Cherenkov experiment that surpasses Milagro in detector area and is located at a higher altitude. The HAWC site at the Sierra Negra mountain in Mexico is at $4100m$ above sea level, where about six times more electromagnetic particles are expected in an EAS compared to the Milagro site at $2600m$. This lowers the energy-threshold of the gamma-ray induced showers that can be observed with the detector to about $100GeV$. Besides the altitude, the site was also chosen because the field of view overlaps with the regions observed by other experiments and because up-to-date site infrastructure like power supply was already developed for the Large Millimeter Telescope at the same mountain a few years earlier. [19]

The HAWC collaboration aimed for a water reservoir used as the central detector of the experiment with an area of at least $20,000m^2$ and a depth of at least $5m$. No previous structure existed anywhere in the world that could be reused for that purpose, so a new design had to be made. First drafts were very similar to Milagro and relied on a central water tank with floating PMTs. [20, 21] However, the engineering challenge of building a water reservoir with that size combined with funding constraints and environmental considerations (subsequent use, dismantling of the experiment after its run time, ...) moved the design away from a single water pond and towards an array of small, individual tanks. A modular detector design is able to achieve the same sensitivity as a single water tank detector as long as the water area, PMT-covered area and PMT depth in the water remain the same. It is less expensive in building costs, adjustable to available funding, straightforward to extend, can be easier dismantled at the end of the experiment and there are more possibilities to re-use or recycle the individual tanks. Additionally, there are the advantages of the up-keeping, repairing and servicing being done without shutting down the whole experiment and the construction happening in parallel for the in-

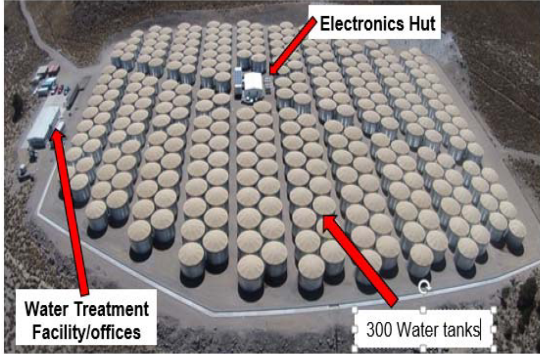


Figure 18: Aerial photograph of the 300 HAWC WCDs covering an area of about $20,000m^2$. From [22]

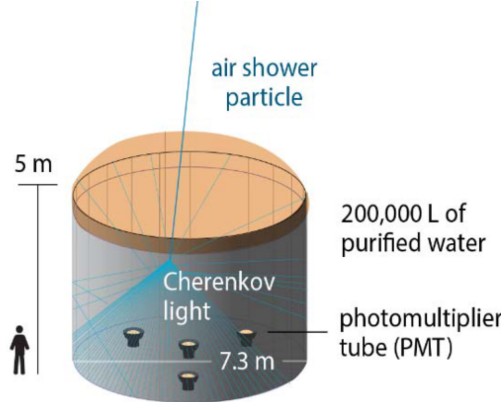


Figure 19: Schematic of a WCD used in HAWC. From [22]

dividual tanks which leads to a shorter construction time and an overall higher run time. [19]

The final design is shown in figure 18. It features 300 water Cherenkov detectors (WCD) in a close packed array covering an area of about $20,000m^2$ (295 are operational). Each WCD (figure 19) is made from a corrugated steel tank with a diameter of $7.3m$ and a height of $5.4m$ filled with $188,000l$ of purified water inside a light-tight plastic bladder. This corresponds to a fill height of about $4.5m$. At the bottom of the WCD are four PMTs, three $20cm$ Hamamatsu R5912 PMTs re-used from Milagro and a central $25cm$ R7081-MOD PMT with a higher quantum efficiency. [19, 22, 23]

Detector Operation and Performance

The data acquisition system of HAWC is highly based on the techniques developed for its predecessor Milagro. HAWC re-uses its electronic components to continuously read-out the PMTs; a PMT is considered hit when the amount of light recorded surpasses a single photon threshold. In contrast to Milagro, where the pulse shape over time for each individual PMT was recorded, HAWC only saves the time for which the light recorded by a PMT surpasses a pre-set threshold. The whole detector read-out is triggered when 28 or more PMT hits are registered in a coincidence window of $150ns$. This corresponds to a trigger rate of about $25kHz$. The raw detector data of about $500MB/s$ is processed in real time which includes the reconstruction of the shower core and shower direction as well as applying background suppressions. Around $20MB/s$ are permanently saved for physics analysis. [24, 25]

In contrast to Milagro, where the limited area required the installation of a second layer of PMTs to provide adequate measurements for background-signal-distinction,

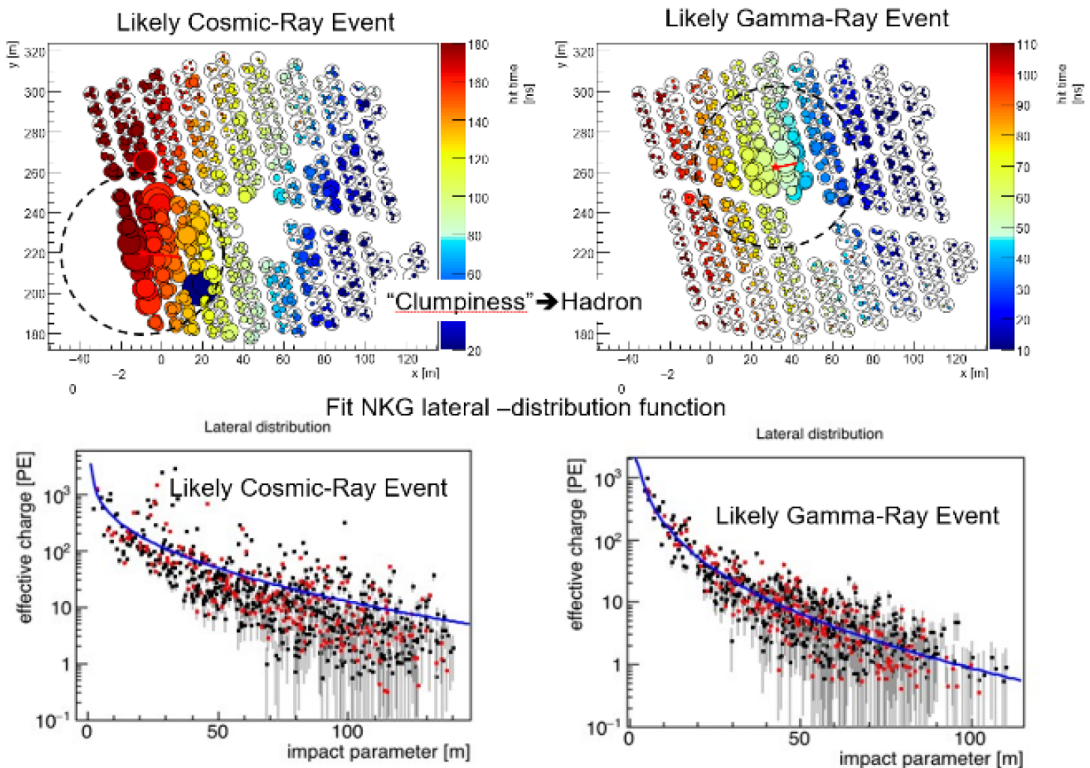


Figure 20: Comparison of a background hadronic shower (left) and a gamma-ray induced electromagnetic shower (right). Cosmic-ray showers include muons and hadrons, which leave a clumpier charge deposit structure in the detector (top row). The lateral shower distribution (bottom row) for background events gives a worse fit to a Nishimura-Kamata-Greisen function. From [22]

the large detector area of HAWC allows for new background rejection techniques based on a single layer of PMTs. The identification of background hadronic showers from cosmic rays relies on identifying the presence of deeply-penetrating particles like hadrons and muons. This can be done by measuring the clumpiness of a shower, meaning the presence of high energy deposits away from the shower core, or by evaluating the lateral shower distribution, which gives a better fit to the Nishimura-Kamata-Greisen function for photon induced showers. Both methods are illustrated in figure 20. [22]

HAWC surpasses Milagro not only in the detector area, but also is located at a higher altitude and introduces a separation of the individual PMTs (which reduces the number of PMTs hit by light traveling horizontally). Overall, these improvements result in a sensitivity gain of factor 15 compared to Milagro. Figure 21 shows a comparison of individual parameters of the two experiments. HAWC has a lower energy threshold of 100GeV than Milagro (250GeV) and a larger effective area at lower energies. The fall of the effective area with lower energy occurs as lower-energy gamma-rays tend to interact with the atmosphere at lower altitudes which results in fewer secondary particles that reach the ground. The larger area allows for the detection of more shower particles, which improves the background rejection efficiency. With higher energy the background rejection efficiency increases and above a primary particle energy of 10TeV observations are basically background-free and only limited by flux. Additionally, the larger detection area results in a better fit of the shower front because its curvature and core location can be determined more precisely. Accordingly, the angular resolution of HAWC is improved and reaches a minimum of 0.25° at primary particle energies above 5TeV . In contrast to Milagro, where the resolution of the reconstructed primary particle energy depends on the localization of the shower core, in HAWC it is only limited by fluctuations in the shower development in the atmosphere that make it impossible to distinguish between a low-energy gamma-ray interacting in the lower atmosphere and a high-energy photon inducing a shower high in the atmosphere. Showers above 30TeV can be reconstructed with a 30% resolution. [19]

Outrigger Array

In 2018, the main WCD array of HAWC was complemented with an outrigger array of 345 small WCDs, separated with a distance between $12m$ and $18m$ (figure 22). Each outrigger detector consists of a water-filled tank with a diameter of $1.55m$ and a height of $1.65m$ equipped with an upwards-facing 20cm Hamamatsu R5912 PMT at the bottom. The installation of the outrigger array extends the instrumented

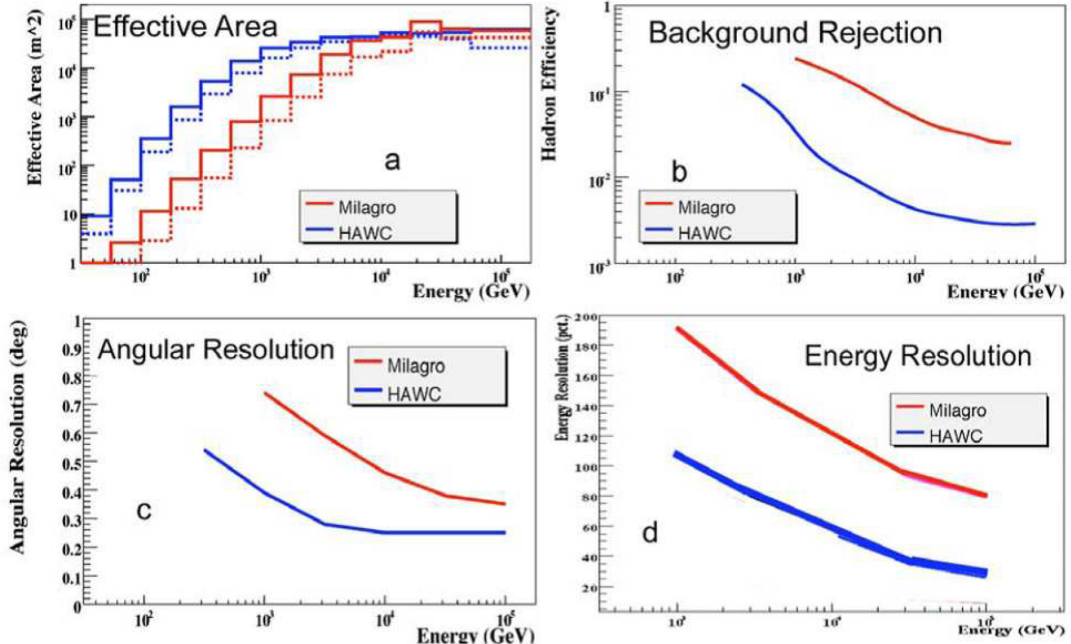


Figure 21: Comparison of the effective area with (dashed) and without (solid) hadron rejection, efficiency of the background rejection, angular resolution and energy resolution between Milagro and HAWC. From [19]

area by a factor of 4 to about $100,000\text{m}^2$. The additional data from the outrigger detectors (figure 23) helps in improving the reconstruction of EAS with cores far outside the main WCD array, but the outrigger's main task is in increasing the effective area of HAWC for energies above 10TeV : At a primary particle energy of around 10TeV the shower size at the altitude of the experiment is comparable to the size of the main detector area. Without the outrigger array, most shower particles would fall outside the detector which makes the shower reconstruction less accurate or impossible. The participation of outrigger WCDs in events in dependence of the primary particle energy is shown in figure 24. Since the energy resolution of HAWC is relatively broad, analyses are binned in fraction of PMTs hit in an event and not directly in the reconstructed particle energy (figure 25). A higher analysis bin with more participating PMTs will correspond to a higher primary particle energy. Figure 24 shows how with a higher bin number the average number of outrigger WCDs hit as well as the fraction of outrigger array participation in the recording of an event grows. [18, 26]

Scientific Results

HAWC has a relatively large field of view of 1.8sr and over the course of a day samples 67% of the sky (figure 26). Hence, observations of gamma-ray sources

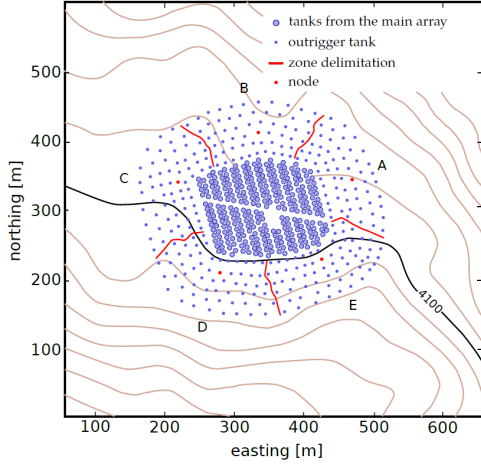


Figure 22: Locations of the 345 outrigger detectors around the HAWC WCD array. From [18]

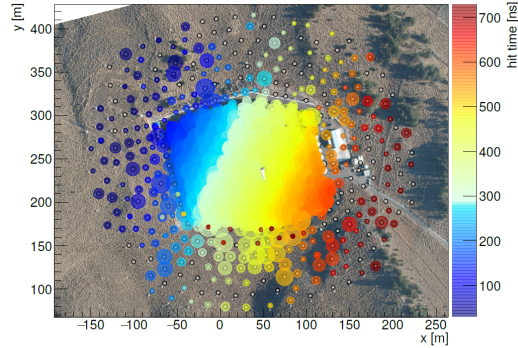


Figure 23: Example of an event that triggered the main array and the outrigger in HAWC. The colors correspond to the time the PMTs at the locations were hit. From [18]

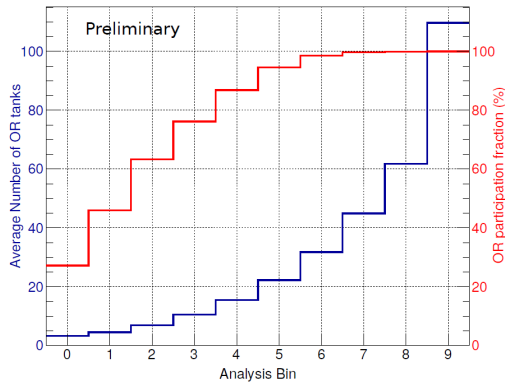


Figure 24: Average number of outrigger WCDs hit (blue) and fraction of outrigger participation (red) in an event depending on the bin number which corresponds to the particle energy. From [18]

Bin	f_{hit} bounds (% of PMTs hit)
1	6.7-10.5
2	10.5-16.2
3	16.2-24.7
4	24.7-35.6
5	35.6-48.5
6	48.5-61.8
7	61.8-74.0
8	74.0-84.0
9	84.0-100.0

Figure 25: Definition of analysis bins used in HAWC. Because of the broad energy resolution of HAWC, analyses are binned in fraction of PMTs hit instead of the reconstructed primary particle energy. From [26]

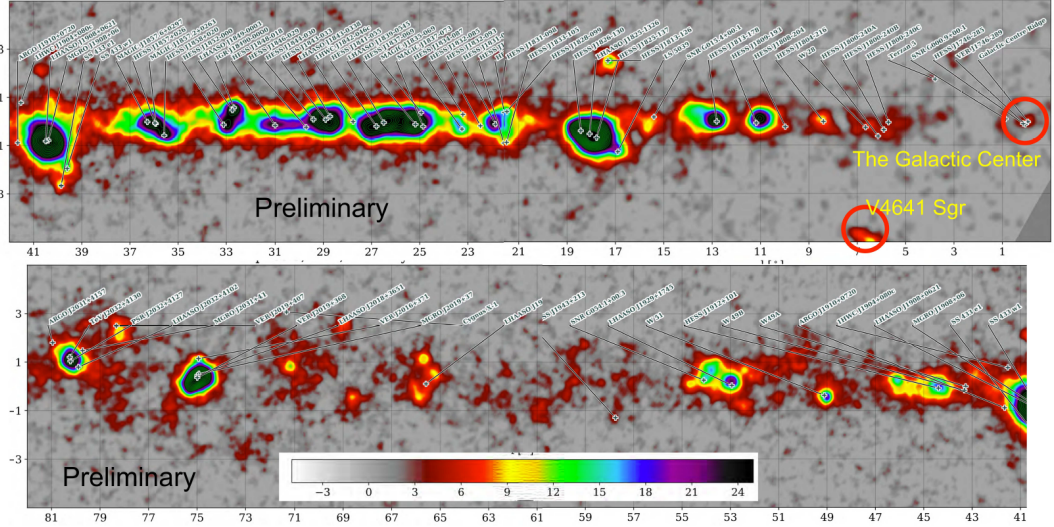


Figure 26: Significance map of the galactic plane as observed by HAWC in 2090 days of operation. The color bar represents the significance in standard deviations. From [29]

made by other experiments can be confirmed and studied in more detail and up to higher energies. HAWC also detected a large number of previously unknown sources and a whole new class of TeV emission sources, halos around pulsars. These are electrons and positrons that escape a pulsar wind nebulae, but remained trapped in an area around. Cosmic microwave background photons can be accelerated from these high-energy leptons via inverse Coulomb scattering. Additionally, HAWC is searching for high-energy gamma-rays in the PeV region and investigating several source candidates. Its results are also being combined with other experiments for multimessenger observations, for example in the search for gamma-ray counterparts of gravitational wave or neutrino events. HAWC used high-energy gamma-rays to test Lorentz invariance violations. It placed a new limit on the energy scale at which Lorentz invariance can possibly occur, $2.2 \cdot 10^{31} eV$, which corresponds to an improvement of 2 orders of magnitude to previous limits. Besides high-energy gamma-ray astronomy, HAWC can be used for cosmic ray physics. [27, 28, 29] HAWC started taking data in 2016 and the first experimental results were used to improve the data processing mechanisms. The experiment is still running and more results can be expected in the next years. [29]

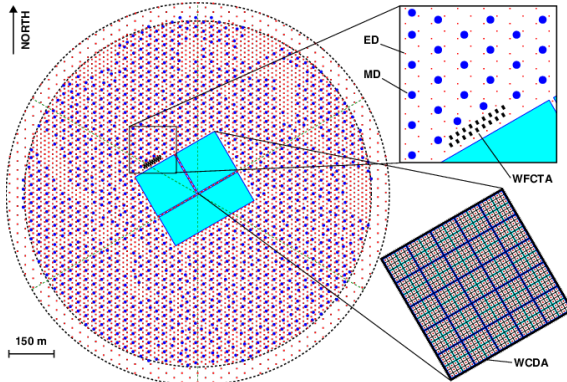


Figure 27: Schematic view of the LHAASO experiment with a water Cherenkov detector array (LHAASO-WCDA), an ACT array (LHAASO-WFCTA) and an EAS array consisting of electromagnetic particle detectors (ED) and muon detectors (MD). From [30]

4 The LHAASO Experiment

The **L**arge **H**igh **A**ltitude **A**ir **S**hower **O**bservatory is located at an altitude of 4410m in the Sichuan province of China. In contrast to Milagro and HAWC, which solely rely on the water Cherenkov technique, LHAASO uses all ground-based methods for EAS detection. It combines an EAS array, LHAASO-KM2A, with a water Cherenkov detector, LHAASO-WCDA, and an ACT array, LHAASO-WFCTA (figure 27). The experiment started collecting data for LHAASO-WFCTA and LHAASO-KM2A in 2019 and scientific results for the two experiment parts have been published. For LHAASO-WCDA, currently only one out of three water Cherenkov tanks has been build and only preliminary studies of the detector operation have been published. [30, 31]

The LHAASO-KM2A experiment is a EAS array with electromagnetic particle detectors (ED) and muon detectors (MD) that focuses on detecting high-energy gamma rays above 100TeV . Each EDs (figure 28) is made out of a plastic scintillation tile with an area of 1m^2 . It is covered with a 5mm-thick lead plate which absorbs low-energy particles in the EAS and converts high-energy shower photons into electron-positron pairs. Wave-length shifting fibres in the scintillation plate collect the light generated by charged particles and guide it to a 3.8cm PMT. In total, 5195 EDs are spread over an area of 1km^2 in a triangular grid. The EDs provide information on the direction and energy of the EAS as well as the location of the shower core. This allows for the reconstruction of the primary particle direction with an angular resolution of 0.3° at 100TeV as well as the primary particle energy with a resolution of 25% at 100TeV . The other component of LHAASO-KM2A are the muon detectors (MD), which help in identifying cosmic rays through probing the presence of muons.

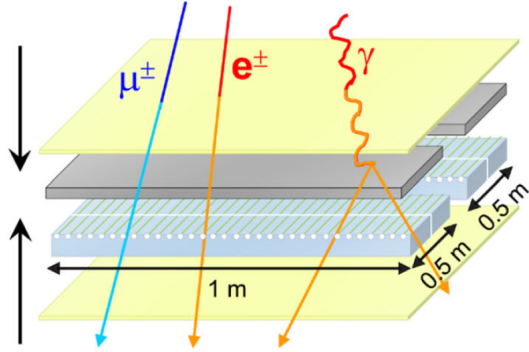


Figure 28: Schematic of the electromagnetic particle detectors in LHAASO-KM2A. From [30]

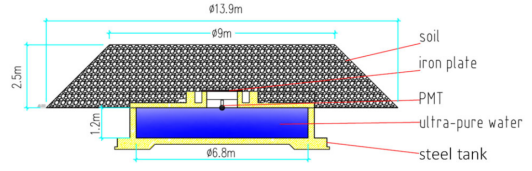


Figure 29: Schematic of the muon detectors in LHAASO-KM2A. From [30]

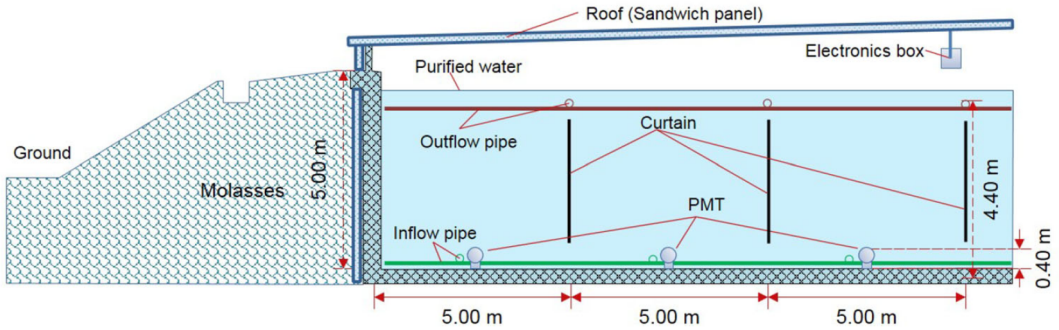


Figure 30: Schematic view of LHAASO-WCDA, the water Cherenkov detector tanks of the LHAASO experiment. From [30]

With the given detector area and duty cycle, the expected number of gamma-rays with an energy above 100TeV is in the order of 10 per year. The MDs provide a possibility of background identification for LHAASO-KM2A that keeps the acceptance to gamma-ray-induced showers high. Besides the background-rejection for gamma-ray astronomy, the MDs are also used to investigate cosmic-ray showers. There are 1171 individual MDs (figure 29), each consisting of a water-filled steel tank with a diameter of 6.8m and a height of 1.2m . The tanks are buried under 2.5m of soil which attenuates all other particles and ensures that only muons reach the water, where they emit Cherenkov light which gets detected by a 20cm-PMT looking down into the water tank. [30]

LHAASO-WCDA (figure 30) is the water Cherenkov detector of the LHAASO experiment, which focuses on gamma-rays with energies between 100GeV and 20TeV . It consists out of three water tanks with a total area of $78,000\text{m}^2$ and a water depth of 4m . The tanks are separated by light-tight plastic curtains into 3000 $5\text{m} \times 5\text{m}$ cells. At the bottom of each cell is a 20cm-PMT which looks upward to detect

Cherenkov light emitted by particles from the EAS. [30]

The LHAASO experiment also features an array of 18 atmospheric Cherenkov telescopes, called LHAASO-WFCTA. It is primarily meant to investigate showers induced by cosmic-rays with energies above $10TeV$, but for gamma-ray astronomy it can be used in combination with LHAASO-KM2A to cross-measure the energy of primary gamma-rays. Each telescope has a spherical light collector of $4.7m^2$ and a focal plane camera with 32×32 pixels made out of a PMT array. In addition to the Cherenkov light produced by particles moving through the atmosphere the telescope can be used to detect fluorescence light emitted by molecules in the atmosphere after the excitation by high-energy photons in EAS. [30, 32]

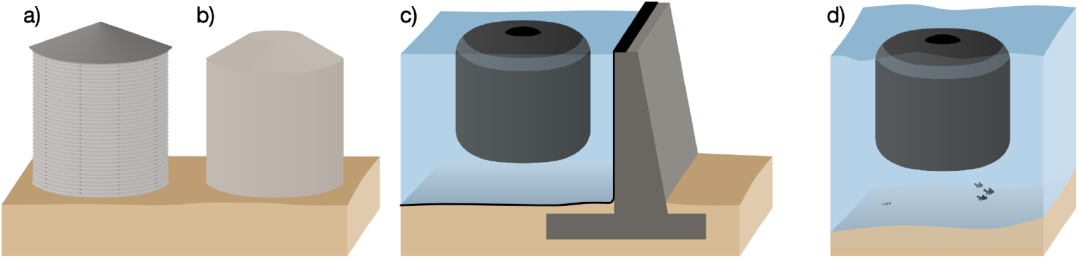


Figure 31: Different possible detector concepts for SWGO: Cylindrical tanks from a) steel or b) plastic; c) water reservoir with individual detector cells ; d) natural lake with floating detector bladder. From [34]

5 The SWGO Experiment

The **Southern Wide-field Gamma-ray Observatory** (SWGO) collaboration aims to build a water Cherenkov detector in the southern hemisphere, as the two currently operating water Cherenkov detectors, HAWC and LHAASO, are both located in the northern hemisphere. The project is in the early planning stage. Possible sites are being evaluated with respect to the site location, altitude, topology and environment, site access, and the availability of water, power and network connectivity. In parallel, detector studies are on-going and different possible detector design are shown in figure 31. It would be possible to use an array of individual water-filled tanks like in the HAWC experiment or a large water reservoir separated into individual cells like LHAASO-WCDA. Individual tanks have the advantage that the only site adaptation needed is the leveling of the ground which in contrast to building a large water reservoir is less expensive, less invasive to the surrounding nature and easier to deconstruct after the experiment. Different tank materials are considered: steel tanks can be produced and shipped inexpensively as packed sheets but have to be assembled on-site; plastic tanks which have to be produced close to the experiment site to become cost-effective. Next to these two designs, the collaboration considers deploying detector units filled with pure water directly in to a natural lake. Using pre-existing lakes provides a design that minimally alters the natural environment and is easiest to deconstruct after the experiment. However, it requires a suitable site and comes with the engineering challenges of constructing and stabilizing the swimming detector bubble. The background rejection in SWGO will rely on the identification of muons in an EAS as well as high-intensity, strongly localized light deposits that are typical for hadronic showers. Two different approaches are considered, two PMT layers like in Milagro or a single layer similar to HAWC and LHAASO-WCDA. [33, 34]

6 Conclusion

Water Cherenkov detectors were developed in the 1990s as a new method of studying high-energy gamma-rays that combines the advantages of a high duty cycle and large field of view, which previously had been the main reason for using extensive air shower arrays, with a relatively low energy threshold of about 100GeV that before was only provided by atmospheric Cherenkov telescopes. The first generation experiment, Milagro, relied on a water tank instrumented with two layers of PMTs and supplemented by an outrigger array of small water Cherenkov detectors in the surrounding area. Based on its success in discovering new high-energy gamma-ray sources and source classes, the second generation detector, HAWC, was developed. HAWC has an increased detector area of about four times the size of the Milagro pond, and is located at a higher altitude, which lowers the energy threshold from 250GeV at Milagro to about 100GeV for HAWC and improves the sensitivity as well as the angular and energy resolution. Due to engineering constraints, HAWC is built in an array design of individual tanks with a single layer of PMTs. HAWC further improved the observations of astrophysical high-energy gamma-ray sources and since the data analysis is still ongoing, more results are to be expected.

Two future water Cherenkov experiments are currently being built and planned: The LHAASO experiment is an impressive project combining all forms of ground-based high-energy gamma-ray observation techniques. The water Cherenkov detector of the experiment, LHAASO-WCDA, has been partially built and so far only preliminary data processing studies have been published. Complementary to HAWC and LHAASO in the northern hemisphere, the SWGO collaboration aims to build a water Cherenkov detector in the Southern hemisphere. The experiment is currently in the planning stages, scouting for possible detector sites and evaluating different detector designs.

In summary, the water Cherenkov technique for detecting high-energy gamma-rays has been proven to be very successful and with HAWC, LHAASO and SWGO three experiments will continue to probe astrophysical gamma-rays to answer fundamental question about the structure of the universe and the objects in it.

7 Bibliography

- [1] Bernard Degrange and Gérard Fontaine. “Introduction to high-energy gamma-ray astronomy”. In: *Comptes Rendus Physique* 16.6-7 (Aug. 2015), pp. 587–599. DOI: <https://doi.org/10.1016/j.crhy.2015.07.003>.
- [2] Giuseppe Di Sciascio. “Ground-based Gamma-Ray Astronomy: an Introduction”. In: *Journal of Physics: Conference Series* 1263.1 (June 2019), p. 012003. DOI: <https://doi.org/10.1088/1742-6596/1263/1/012003>.
- [3] J. F. McCullough and The Milagro Collaboration. *Status of the Milagro Gamma Ray Observatory*. 1999. DOI: <https://doi.org/10.48550/arXiv.astro-ph/9906383>.
- [4] G Sinnis. “Air shower detectors in gamma-ray astronomy”. In: *New Journal of Physics* 11.5 (May 2009), p. 055007. DOI: <https://doi.org/10.1088/1367-2630/11/5/055007>.
- [5] Gaurang B. Yodh and The Milagro Collaboration. “The Milagro Gamma Ray Observatory”. In: *International Symposium on Cosmic Ray Physics in Tibet*. Tibet University, 1994, pp. 39–50. URL: <https://inspirehep.net/literature/1651369>.
- [6] A. J. Smith and The Milagro Collaboration. “The Milagro Gamma-Ray Observatory”. In: *Proceedings of the 29th International Cosmic Ray Conference*. 2005, pp. 227–241. URL: <https://adsabs.harvard.edu/full/2005ICRC...10..227S>.
- [7] Jordan A Goodman and The Milagro Collaboration. “Study of Galactic Gamma-Ray Sources with Milagro”. In: *Journal of Physics: Conference Series* 60 (Mar. 2007), pp. 123–126. DOI: <https://doi.org/10.1088/1742-6596/60/1/022>.
- [8] New York University Experimental Particle Physics Group. “A brief history of Milagro”. 2021. URL: <https://physics.nyu.edu/experimentalparticle/milagro.html>.
- [9] The Milagro Collaboration. “Status of the Milagro Gamma Ray Observatory”. In: (2001). DOI: <https://doi.org/10.48550/arXiv.astro-ph/0110513>.
- [10] J. E. McEnery and The Milagro Collaboration. “The Milagro Gamma-Ray Observatory”. In: *AIP Conference Proceedings*. 2001. DOI: <https://doi.org/10.1063/1.1370821>.
- [11] J. A. J. Matthews. “Lessons learned from Milagro Outrigger Detectors”. 2006. URL: https://nmcpp.unm.edu/auger_north_ucolorado.pdf.

- [12] Gus Sinnis. “Water Cherenkov technology in gamma-ray astrophysics”. In: *Nuclear Instruments and Methods in Physics Research Section A: Accelerators, Spectrometers, Detectors and Associated Equipment* 623.1 (Nov. 2010), pp. 410–412. DOI: <https://doi.org/10.1016/j.nima.2010.03.019>.
- [13] The Milagro Collaboration. “TeV Gamma-Ray Sources from a Survey of the Galactic Plane with Milagro”. In: *The Astrophysical Journal* 664.2 (July 2007), pp. L91–L94. DOI: <http://doi.org/10.1086/520717>.
- [14] The Milagro Collaboration. “Milagro Observations of Multi-TeV Emission From Galactic Sources in the Fermi Bright Source List”. In: *The Astrophysical Journal* 700.2 (July 2009), pp. L127–L131. DOI: <http://doi.org/10.1088/0004-637X/700/2/L127>.
- [15] The Milagro Collaboration. “A Measurement of the Spatial Distribution of Diffuse TeV Gamma-Ray Emission from the Galactic Plane with Milagro”. In: *The Astrophysical Journal* 688.2 (Dec. 2008), pp. 1078–1083. DOI: <http://doi.org/10.1086/592213>.
- [16] The Milagro Collaboration. “The Large-Scale Cosmic-Ray Anisotropy as observed with Milagro”. In: *The Astrophysical Journal* 698.2 (June 2009), pp. 2121–2130. DOI: <http://doi.org/10.1088/0004-637X/698/2/2121>.
- [17] The HAWC Collaboration. “Sensitivity of the High Altitude Water Cherenkov Detector to Sources of Multi-TeV Gamma Rays”. In: (2013). DOI: <https://doi.org/10.48550/arXiv.1306.5800>.
- [18] Vincent Marandon, Armelle Jardin-Blicq, and Harm Schoorlemmer. “Latest News from the HAWC Outrigger Array”. In: (2019). DOI: <https://doi.org/10.48550/arXiv.1908.07634>.
- [19] M.M. Gonzalez. “The High Altitude Water Cherenkov Observatory, HAWC. Designand Performance”. In: *Proceedings of the 31st ICRC, LODZ, 2009.* 2009. URL: <https://srl.utu.fi/AuxDOC/kocharov/ICRC2009/pdf/icrc0863.pdf>.
- [20] The HAWC Collaboration. *HAWC @ México. Un Observatorio de Rayos Gamma de Gran Altura*. Tech. rep. 2007. URL: https://www.hawc-observatory.org/publications/docs/protocolo_55155a.pdf.
- [21] The HAWC Collaboration. *The HAWC Experiment at the Parque Nacional Pico de Orizaba*. Tech. rep. 2007. URL: <https://www.hawc-observatory.org/publications/docs/repfin.pdf>.

- [22] R.W. Springer. “The High Altitude Water Cherenkov (HAWC) Observatory”. In: *Nuclear and Particle Physics Proceedings* 279-281 (Oct. 2016), pp. 87–94. DOI: <https://doi.org/10.1016/j.nuclphysbps.2016.10.013>.
- [23] The HAWC Collaboration. “HAWC as a Ground-Based Space-Weather Observatory”. In: *Solar Physics* 296.6 (June 2021). DOI: <https://doi.org/10.1007/s11207-021-01827-z>.
- [24] The HAWC Collaboration. *On the Sensitivity of the HAWC Observatory to Gamma-Ray Bursts*. 2011. DOI: <https://doi.org/10.48550/arXiv.1108.6034>.
- [25] The HAWC Collaboration. “Data acquisition architecture and online processing system for the HAWC gamma-ray observatory”. In: *Nuclear Instruments and Methods in Physics Research Section A: Accelerators, Spectrometers, Detectors and Associated Equipment* 888 (Apr. 2018), pp. 138–146. DOI: <https://doi.org/10.1016/j.nima.2018.01.051>.
- [26] The HAWC Collaboration. “Searching for Dark Matter Sub-Structure with HAWC”. In: *Journal of Cosmology and Astroparticle Physics* 2019.07 (July 2019), pp. 022–022. DOI: <https://doi.org/10.1088/1475-7516/2019/07/022>.
- [27] Petra Huentemeyer. “Latest Results from the HAWC-Observatory”. XXVIII Cracow EPIPHANY Conference on Recent Advances in Astroparticle Physics. Jan. 2022. URL: <https://indico.cern.ch/event/1034990/contributions/4663419/attachments/2370607/4048650/Epiphany2022-PHH.pdf>.
- [28] The HAWC Collaboration. “Constraints on Lorentz Invariance Violation from HAWC Observations of Gamma Rays above 100 TeV”. In: *Physical Review Letters* 124.13 (Mar. 2020), p. 131101. DOI: <https://doi.org/10.1103/PhysRevLett.124.131101>.
- [29] Omar Tibolla. “Recent results from the HAWC experiment”. In: *Journal of Physics: Conference Series* 2429.1 (Feb. 2023), p. 012017. DOI: <http://doi.org/10.1088/1742-6596/2429/1/012017>.
- [30] Huihai He and. “Design of the LHAASO detectors”. In: *Radiation Detection Technology and Methods* 2.1 (Feb. 2018). DOI: <https://doi.org/10.1007/s41605-018-0037-3>.
- [31] Mingjun Chen and. “Status and First Result of LHAASO-WCDA”. In: *Proceedings of 36th International Cosmic Ray Conference — PoS(ICRC2019)*. Sissa Medialab, Aug. 2020. DOI: <https://doi.org/10.22323/1.358.0217>.

- [32] The LHAASO Collaboration. “Construction and on-site performance of the LHAASO WFCTA camera”. In: *The European Physical Journal C* 81.7 (July 2021). doi: <https://doi.org/10.1140/epjc/s10052-021-09414-z>.
- [33] Jim Hinton. *The Southern Wide-field Gamma-ray Observatory: Status and Prospects*. 2021. doi: <https://doi.org/10.48550/arXiv.2111.13158>.
- [34] Felix Werner and Lukas Nellen. “Technological Options for the Southern Wide-Field Gamma-Ray Observatory (SWGO) and Current Design Status”. In: *Proceedings of 37th International Cosmic Ray Conference ICRC 2021*. Sissa Medialab, July 2021. doi: <https://doi.org/10.22323/1.395.0714>.